Optical Properties and Dispersion Parameters of PAAm-PEG Polymer Blend Doped with Antimony (III) Oxide Nanoparticles

Ahed Ali Kadhim Zbala[1], Abdulazeez O. Mousa Al-Ogaili[2], Khalid Haneen Abass[3*]

Abstract

Oxide of antimony (III) (Sb_2O_3) is a type of amphoteric oxide, is used in a variety of applications is a pacifying agent for glasses, ceramics, enamels, catalyst, production of plastic, and the vulcanization of rubber. Polymer blend films were prepared by mixing polyacrylamide (PAAm) and polyethylene glycol (PEG4000), with different contents of Sb_2O_3 nanoparticles by casting method. The diffusions of Sb_2O_3 nanoparticles within the mixture were examined using optical microscopy. The optical microscopic images showed that good diffusions of nanoparticles with some agglomerations. The optical characteristics were studied by the Spectrophotometer for ultraviolet and visible light in the range of (200-1100) nm. Most optical properties increased with the increasing of wavelength except for transmittance and energy gaps. The analysis of optical properties is the focus of this paper of (PAAm-PEG-Sb_2O_3) nanocomposite polymer films and study the (Dispersion energy)Ed, (single oscillator energy)Eo, (static refraction index)n(0), and (Moments) M-1 and M-3 are examples of dispersion parameters.

Key Words: Nanocomposite, PAAm, Optical Properties, Dispersion Parameters.

DOI Number: 10.14704/nq.2022.20.2.NQ22026 **NeuroQuantology 2022; 20(2):62-68**

Introduction

Polymer composites are widely used in various aspects of industrial, medical, biological, and opto-electrical applications. It has many advantageous properties, as in resistance, mechanical characteristics, and price-effectiveness, which make it the polymer of choice for a wide range of applications (Singh *et al*, 2003). Scientists are working hard to develop high-quality polymer composites for use in modern applications. Polymer composites research is expanding rapidly in a variety of exciting directions (Elf strand *et al*, 2009). Because they have better properties than original polymers, polymer blends play an important role in the development of new materials (Ibrahim and Kadum, 2010; Al-Jamal *et al*, 2019; Abass and Hamed, 2020; Abass *et al,* 2021). The property of the material (internal structure) is one of the key factors and has a direct effect on the synthesized nanocomposites, as the nan-fillers in the matrix and the polymer have a strong interaction penny. In addition, it is important for the stability and scattering of the nan-filler in the polymer matrix. This can significantly improve the properties of polymer nanocomposites (Layek and Nandi, 2014; Jawad *et al*, 2011). There are two factors that control the mechanical properties of polymers (McCrum and Bucknall, 1997): the first factor is the length of the molecule, which is proportional to n (determining the number of monomers), and proportional to the molecular size, or relative molecular mass.

Corresponding author: Khalid Haneen Abass
Address: [1]Department of Physics, College of Science, University of Babylon, Iraq; [2]Department of Physics, College of Science, University of Babylon, Iraq; [3*]Department of Physics, College of Education for Pure Sciences, University of Babylon, Iraq.
E-mail: [1]ahad.zballa.scihigh80@student.uobabylon.edu.iq; [3*]pure.khalid.haneen@uobabylon.edu.iq
Relevant conflicts of interest/financial disclosures: The authors declare that the research was conducted in the absence of any commercial or financial relationships that could be construed as a potential conflict of interest.
Received: 09 December 2021 **Accepted:** 12 January 2022

The second factor is the shape or structure of the molecule. Oxide of antimony (III) is a chemical compound that is inorganic. They occur naturally as valentine minerals and cinarmontite (Greenwood and Earnshaw, 2012).

Like most polymeric oxides, Sb_2O_3 dissolves in an aqueous solution. Arsenic oxide and antimony coexist in nature as a very rare mineral (Naser *et al*, 2020). This semiconductor group includes Sb_2O_3. It is a very interesting material in basic science. Research and technical applications due to its structural, optical, electrical and photo-electronic properties (Kiriakidis *et al*, 2000). Sb_2O_3 consumption there are approximately 10,000 and 25,000 in the United States and Europe, respectively tons per year, respectively. The primary application is as a synergist fire-retardant in conjunction utilizing halogenated materials. The combination of halides and antimony contributes to the flame retardant effect of polymers, resulting in fewer flammable coal. These fire-retardant can be found in electronics, textiles, leather, and coatings (Abass and Obaid, 2019). In this study, the optical properties and dispersion parameters of PAAm-PEG-Sb_2O_3 nanocomposites were examined to candidate it for optical devices fabrication.

Experimental Method

1. Materials

Two polymers were mixed as a bases material; PAAm and PEG. PAAm was purchased from British Drug Houses (BDH) with purity of (99.99%) and (5×10^6 g/mol) molecular weight. PEG was purchased from EMPROVE ESSENTAL Ph Eur with molecular weight=4000 and assay purity=99%. The doped material was Sb_2O_3 purchased from US Research Nanomaterials, Inc.

2. Synthesis of Nanocomposites

0.75 g PAAm was dissolved in 60 mL of distilled water, stirred at 80°C, and 0.25 g of PEG was added to the solution with stirring at 70°C. Then, Sb_2O_3 was added to the solution with different content (0.02, 0.04 and 0.06) g as shown in table (1) with the same particle size to form the samples. The mixture was mixed for 15 minutes after the nanoparticles additive to obtain a homogeneous mixture and then left for 24 hours before pouring. The solution is placed in a petri dish and allowed to dry at room temperature for 10 days, homogeneity, and distribution of Sb_2O_3 nanoparticles in (PAAm-PEG-Sb_2O_3) films were studied using an optical microscope. Ultraviolet Visible Spectrophotometer, which is used to determine the absorption spectra in the range (190-1100) nm. The resulting samples were prepared with a thickness range (120) µm. Thickness was measured with a digital micrometer.

Table 1. Materials used in the (PAAm-PEG- Sb_2O_3) nanocomposites

PAAm (g)	PEG (g)	Sb_2O_3 (g)
0.75	0.250	0
0.735	0.245	0.02
0.720	0.240	0.04
0.705	0.235	0.06

Results and Discussion

Figure (1) At a magnification of 100X, the optical images of PAAm-PEG and PAAm-PEG-Sb_2O_3 nanocomposites with varying Sb_2O_3 concentrations are shown. These images demonstrated the matrix's fine homogeneity with a favorable distribution of Sb_2O_3 into the polymer composite blends. The optical microscopy (OM) pictures demonstrated that the PAAm-PEG-Sb_2O_3 nanocomposites were successfully prepared using the casting method.

Figure (1-a) represents the PAAm-PEG blend that refer to good dissolving of polymers. The parts (b, c, and d) in figure 1 show the diffusion of Sb_2O_3 in the PAAm-PEG blend. The agglomeration of nanoparticles can see in the part (d) from the figure, which represents the PAAm-PEG-6%Sb_2O_3, refer to the interaction that accurse among Sb_2O_3 nanoparticles because the high value of surface to volume ratio.

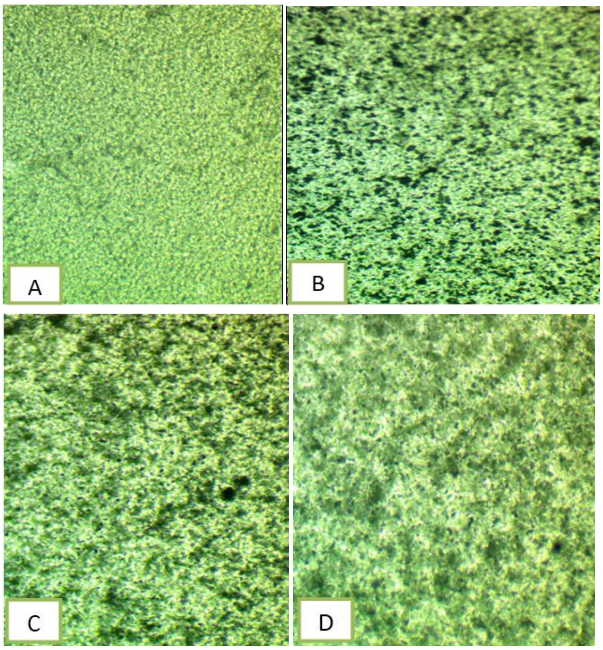

Figure 1. Photomicrographs (100X) of nanocomposites: a) PAAm-PEG, b) PAAm-PEG: 0.02wt.% Sb_2O_3 c) PAAm-PEG:0.04wt.% Sb_2O_3, and d) PAAm-PEG:0.06wt.% Sb_2O_3

The transmittance spectra (T) were calculated using the following relationship (Tuama *et al*, 2020):

$$T = \log A \qquad (1)$$

Where A is absorption. Figure (2) shows transmittance of (PAAm-PEG-Sb_2O_3) nanocomposites with wavelength. As illustrated in the diagram, the transmittance decreases with the rise of Sb_2O_3 nanoparticles. This is caused by the added Sb_2O_3 nanoparticle.

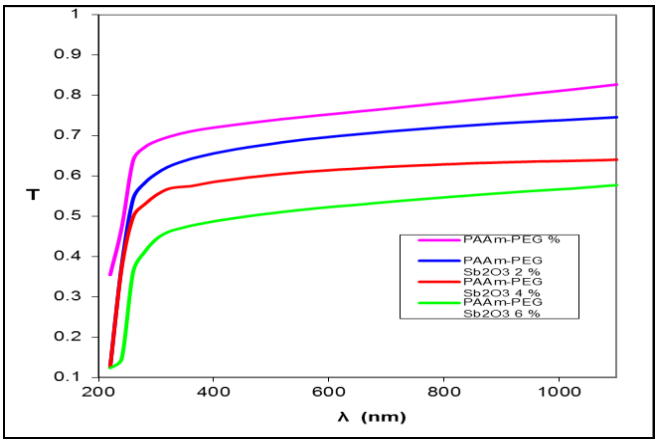

Figure 2. Transmittance behavior of (PAAm-PEG-Sb_2O_3) nanocomposite with various content of Sb_2O_3 NPs

The equation (2) defines the extinction coefficient (k) (Asadi *et al*, 2019; Rasool *et al*, 2020):

$$k = a\lambda/4\pi \qquad (2)$$

Where α is the absorption coefficient and λ is the incident photon wavelength.

Figure (3) shows the relationship between the extinction coefficient and the wavelength of (PAAm-PEG-Sb_2O_3) nanocomposites with various content of Sb_2O_3 NPs. It should be noted that (k) has low worth at low wavelength, but it increases with the increasing of the concentration of the Sb_2O_3 NPs. This is credited to the increased coefficient of absorption with increase of the weight percentages of Sb_2O_3 nanoparticles. The coefficient of extinction has high values at the UV region. This activity was due to all samples high absorbance of nanocomposites. In addition, the extinction coefficient of the nanocomposites increases with increasing of the visible wavelength and the near-infrared wavelengths, which are these, due to the absorption coefficient of the nanocomposites, which is nearly constant in the visible and near-infrared ranges, so increases extinction coefficient as wavelength increases. This result is consistent with the researchers in the reference (Kadhim, 2016).

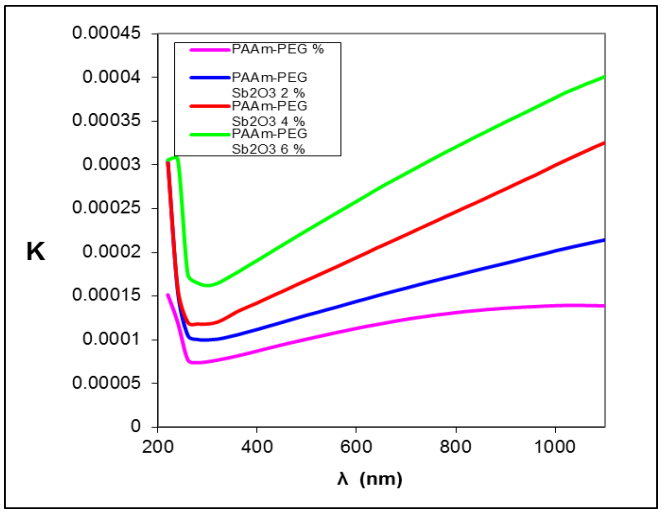

Figure 3. Variation of extinction coefficient of (PAAm-PEG-Sb_2O_3) nanocomposite with various content of Sb_2O_3 NPs

The equation (3) determines the refractive index (n) of Sb_2O_3 films (Bassani and Parravicini, 1975; Khadayeir *et al*, 2018):

$$n = 1 + R / 1 - R + [4R / (1 - R)^2 - k^2] \qquad (3)$$

Figure (4) represents the connection between the refractive index and the wavelength with various content of Sb_2O_3 NPs. According to the graph, the refractive index fell as the content of Sb_2O_3 NPs increased where R is reflectance.

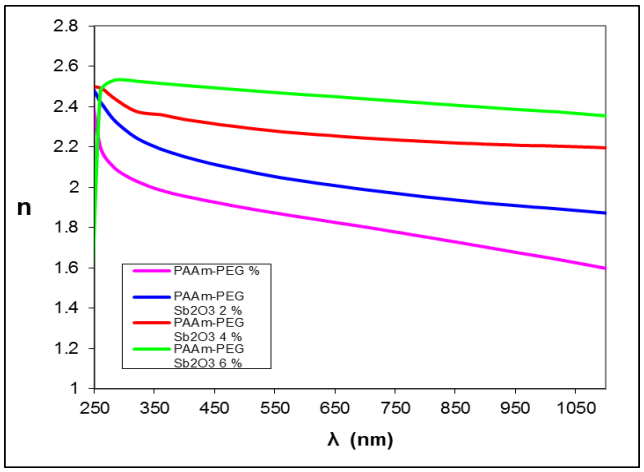

Figure 4. Variation of refractive index with wavelength of (PAAm-PEG-Sb_2O_3) nanocomposite with various content of Sb_2O_3 NPs

The absorption coefficient ($\boldsymbol{a}$) can be calculated using (Abass *et al*, 2018; Al-Aaraji *et al*, 2019; Al-Aaraji *et al*, 2019):

$$a = (2.303A)/t \qquad (4)$$

A and t refer to the absorbance and the thickness of samples respectively.

Figure (5) shows the absorption coefficient (α) as a function of photon energy for the (PAAm–PEG) blend with different Sb_2O_3 nanoparticle

concentrations. It is worth noting that at low energy levels, absorption is minimal. This means that the electron transition has occurred unlikely because the incident photon's energy is insufficient to transfer an electron from the valence to the conduction band (hν ≤ Eg). Absorption increases with energy, indicating that electron transitions are more likely; the frequency of the occurrence photon is sufficient to transfer the electron from the valence to the conduction band. This means that the incident photon energy is higher than the permitted energy gap. This demonstrates that the coefficient of absorption aids in determining the electron transition's nature; when the absorption coefficient is high ($\alpha>10^4$) cm^{-1} at high energies, It is anticipated that a direct transition will occur of the electron occurs, electrons and photons keep the moment and energy going.; when the absorption coefficient is low ($\alpha<10^4$ cm^{-1}), it is expected that indirect transition of the electron occurs.

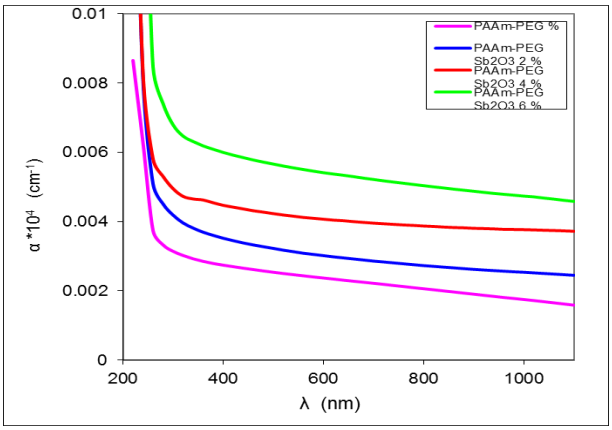

Figure 5. Variation of absorption coefficient (α) of (PAAm-PEG-Sb_2O_3) nanocomposite with various content of Sb_2O_3 NPs

The non-direct transition model of (PAAm-PEG-Sb_2O_3) nanocomposites is described by (Tauc *et al*, 1970):

$$ahv = (hv - E_g) \qquad (5)$$

Where hυ refer to photon energy and E_g the energy gap.

Energy gap of transitions (forbidden and allowed) reduces with the rise in Sb_2O_3 ratios, which related to create localized levels in the optical band gap (Tuama *et al*, 2021; Abass and Mohammed, 2019).

We note from the drawing that the energy gap decreases with the increase of the Sb_2O_3 NPs, as there will be secondary levels between the conduction and the valence band, which will reduce the energy gap.

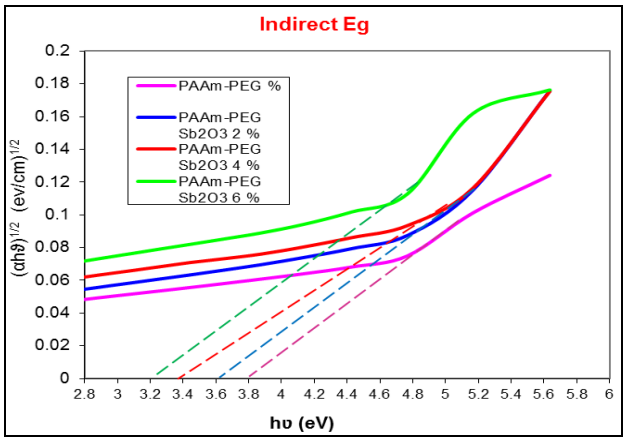

Figure 6. Variation of $(ahv)^{1/2}$ of (PAAm-PEG-Sb_2O_3) nanocomposite with various content of Sb_2O_3 NPs

The real (ε_r) and imaginary (ε_i) parts of dielectric constant for (PAAm-PEG-Sb_2O_3) nanocomposites were determined by using the equations (Nnabuchi, 2006; Abass *et al*, 2018).

$$\varepsilon_r = n^2 - k_o^2 \qquad (6)$$

$$\varepsilon_i = 2nk_o \qquad (7)$$

Figures (7) represent the relationship between real and imaginary dielectric constants in nanocomposites (PAAm-PEG-Sb_2O_3). The figures show that the ε_r and ε_i increased as the concentration of Sb_2O_3 NPs increased.

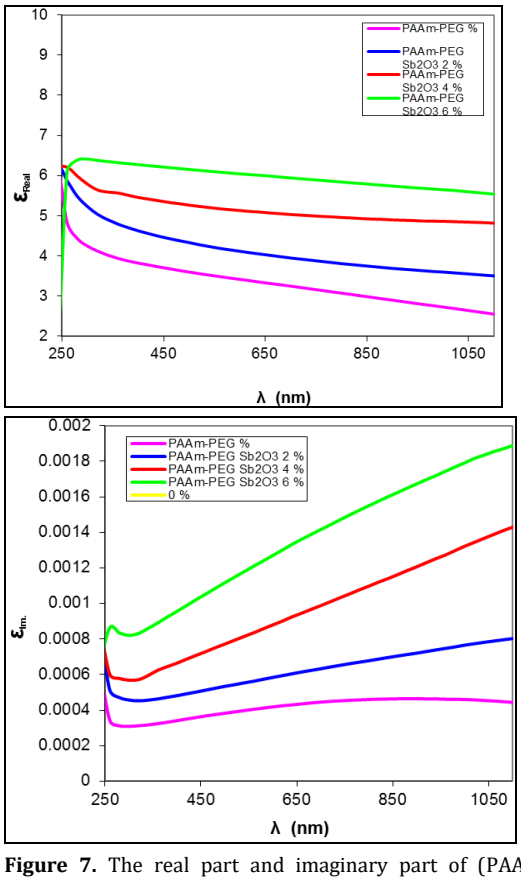

Figure 7. The real part and imaginary part of (PAAm-PEG-Sb_2O_3) nanocomposite with various content of Sb_2O_3 NPs

The dispersion parameters introduced by Wemple-DiDomenico model. For (PAAm-PEG-Sb_2O_3) nancomposites are determined from the relation (Wemple and DiDomenico, 1971):

$$n^2 - 1 = [\, E_d E_o / E_o^2 - (h\upsilon)^2 \,] \quad (8)$$

Where n denotes the refractive index, Eo denotes the oscillator energy, and Ed denotes the dispersion energy as it relates to the average strength of the optical transitions (Sharba *et al*, 2020). These parameters are estimable from $(n^2\text{-}1)^{-1}$ on y-axis and $(h\upsilon)^2$ on x-axis. It can use the slope $(E_oE_d)^{-1}$ and intercept (E_o/E_d). Fig.8 represents the relationship between the $(n^2\text{-}1)^{-1}$ and $(h\upsilon)^2$. The resulted values of E_o and E_d were listed in Table (2). The values of E_o and E_d decrease with the increase of Sb_2O_3 additive in the PAAm-PEG blend. To determine the values of bandgap (E_g), it can be obtained from the relation $E_o \approx 2E_g$ (Ahmed *et al*, 2020), these values are offered in Table (2). The resulted values of energy gaps of the prepared nanocomposites were comparable with the resulted from Tauc model.

The moments of the optical spectra (M_{-1}, M_{-3}) of PAAm-PEG-Sb_2O_3 can determine from the equations (Walton and Moss, 1963; Abass and Latif, 2016):

$$E_o^2 = M_{-1}/M_{-3} \quad (9)$$

$$E_d^2 = M_{-1}^3/M_{-3} \quad (10)$$

The values of the optical spectra moments increased with the increase of Sb_2O_3 additive in the PAAm-PEG blend, as listed in Table (2). The values of energy gap decreased as the nanoparticle content increase, while the values of n(o) and M_{-1}, M_{-3} were increased by increasing Sb_2O_3 NPs. As shown in the figures (8-11).

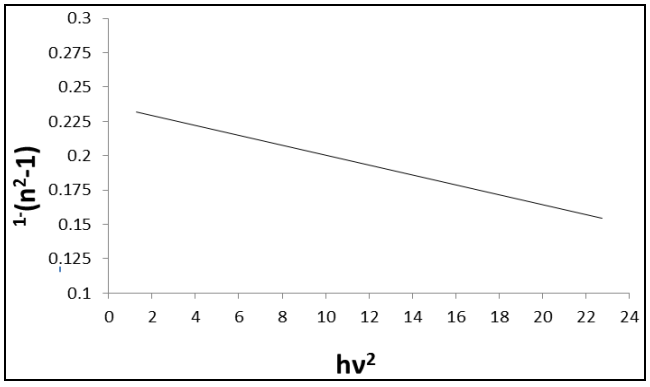

Figure 8. The $(n^2\text{-}1)^{-1}$ versus $(h\upsilon)^2$ of the nanocomposite (PAAm-PEG)

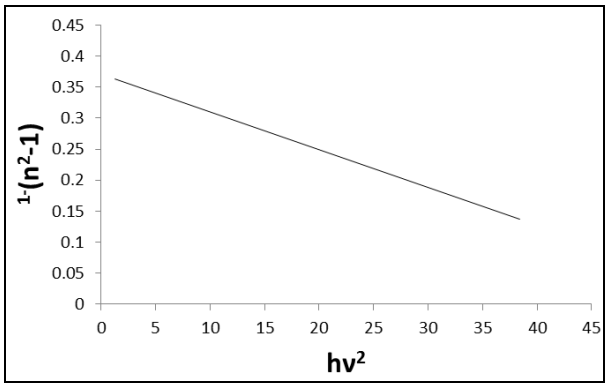

Figure 9. The $(n^2\text{-}1)^{-1}$ versus $(h\upsilon)^2$ of the nanocomposite (PAAm-PEG-Sb_2O_3) with 0.02% of Sb_2O_3 NPs

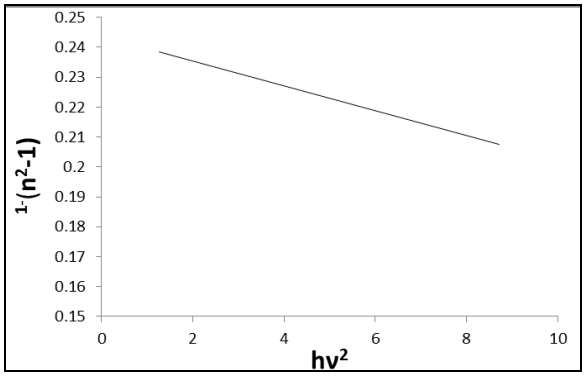

Figure 10. The $(n^2\text{-}1)^{-1}$ versus $(h\upsilon)^2$ of the nanocomposite (PAAm-PEG-Sb_2O_3) with 0.04% of Sb_2O_3 NPs

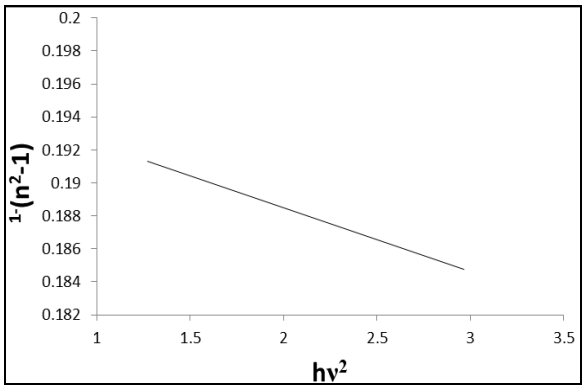

Figure 11. The $(n^2\text{-}1)^{-1}$ versus $(h\upsilon)^2$ of the nanocomposite (PAAm-PEG-Sb_2O_3) with 0.06% of Sb_2O_3 NPs

Table 2. The dispersion parameters and energy gap resulted from Wemple-DiDomenico model of PAAm-PEG-Sb_2O_3

Sample	Pure	0.02wt.%Sb_2O_3 additive	0.04wt.%Sb_2O_3 additive	0.06wt.%Sb_2O_3 additive
E_o	8.21	7.82	7.65	7.27
E_d	34.97	20.85	31.38	37.82
E_g	4.10	3.91	3.82	3.63
n(0)	2.29	1.91	2.25	2.49
E	5.25	3.66	5.09	6.20
M_{-1}	4.25	2.66	4.09	5.20
M-3	0.06	0.04	0.06	0.09

Conclusion

The PAAm–PEG mixture was successfully prepared by casting method. The optical microscopy images showed the wide and homogeneous diffusion of the nanomaterial in the films. The absorption spectra were recorded in the range (190-1100)nm from the Spectrophotometer for UV-visible light. All treatments except the transmittance and the energy gap increased when adding the nanomaterial. By studying the scattering coefficients, We discovered that increasing the nanoparticles in the films reduced dispersion parameters such as E_d, E_o, n(0), S_o, M_{-1}, and M_{-3}. The Wemple-DiDomenico model was used to determine these dispersion parameters to study the possibility used of the prepared nanocomposites in the optical devices.

References

Abass KH, Obaid NH. 0.006 wt.% Ag-Doped $Sb2O_3$ Nanofilms with Various Thickness: Morphological and optical properties. *In Journal of Physics: Conference Series* 2019: 1294(2).

Abass KH, Hamed AH. Reduction of Energy Gap in ZrO_2 Nanoparticles on Structural and Optical Properties of Casted PVA–PAAm Blend. *Journal of Green Engineering* 2020; 10(7): 4166-4176.

Abass KH, Latif DM. The urbach energy and dispersion parameters dependence of substrate temperature of CdO thin films prepared by chemical spray pyrolysis. *International Journal of ChemTech Research* 2016; 9(9): 332-338.

Abass KH, Mohammed MK. Fabrication of ZnO: Al/Si solar cell and enhancement its efficiency via Al-doping. *Nano Biomedicine and Engineering* 2019; 11(2): 170-177.

Abass KH, Adil A, Mohammed MK, Fabrication and enhancement of SnS: Ag/Si solar cell via thermal evaporation technique. *Journal of Engineering and Applied Sciences* 2018; 13(4): 919-925.

Abass KH, Shinen MH, Alkaim AF. Preparation of TiO_2 nanolayers via sol-gel method and study the optoelectronic properties as solar cell application. *Journal of Engineering and Applied Sciences* 2018; 13(22): 9631-9637.

Abass KH, Kadim AM, Mohammed SK, Agam MA. Drug delivery system based on polymeric blend: A Review. *Nano Biomedicine and Engineering* 2021; 13(4): 414-424.

Ahmed FS, Ahmed NY, Ali RS, Habubi NF, Abass KH, Chiad SS. Effects of substrate type on some optical and dispersion properties of sprayed CdO thin films. *NeuroQuantology* 2020; 18(3): 56-65.

Al-Aaraji N, Mousa AO, Naser BA. Spectral and linear optical characterization of Rhodamine B and fluorescein sodium organic laser dyes mixture solutions. *Iraqi Journal of Sciencethis link is disabled* 2019; 60: 69–74.

Al-Aaraji N, Mousa AO, Naser BA. Effect of Polarity of Solvents on Linear Optical Properties for Organic Dye. *Journal of Physics: Conference Series* 2019: 1234(1).

Al-Jamal AN, Hadi QM, Hamood FJ, Abass KH. Particle size effect of Sn on structure and optical properties of PVA-PEG blend. *Proceedings-International Conference on Developments in eSystems Engineering DeSE* 2019: 736-740.

Asadi SMA, Hamood FJ, Abass KH, Mohammed SK, Hassan IM, Latif D. The effect of MGO nanoparticles on structure and optical properties of PVA-PAAm blend. *Research Journal of Pharmacy and Technology* 2019; 12(6): 2768-2771.

Bassani FG, Parravicini GP. Interband transitions and optical properties. *Electronic States and Optical Transitions In Solids* 1975: 149- 176.

Elf Strand L, Elias Son, Dahlgren M. The effect of starch material, encapsulated protein and production conditions on the protein release from starch microspheres. *Journal of pharmaceutical sciences* 2009; 98(10): 3802–3815.

Sharba KS, Alkelaby AS, Sakhil MD, Abass KH, Habubi NF, Chiad SS. Enhancement of urbach energy and dispersion parameters of polyvinyl alcohol with Kaolin additive. *NeuroQuantology* 2020; 18(3): 66-73.

Greenwood NN, Earnshaw A. *Chemistry of the elements*, Elsevier 2012.

Ibrahim BA, Kadum KM. Influence of polymer blending on mechanical and thermal properties. *Modern Applied Science* 2010; 4(9): 157-161.

Jawad E, Khudhair SH, Ali HN. A thermodynamic study of adsorption of some days on iraqi bentoniet modified clay. *European Journal of Scientific Research* 2011; 60(1): 63-70.

Kadhim RG. Study of some optical properties of polystyrene-Copper nanocomposite films. *World Scientific News* 2016; 30: 14-25.

Khadayeir AA, Abass KH, Chiad SS, Mohammed MK, Habubi NF, Hameed TK, Al-Baidhany IA. Study the influence of Antimony Trioxide (Sb_2O_3) on optical properties of (PVA-PVP) composite. *Journal of Engineering and Applied Sciences* 2018; 13(22), 9689-9692.

Kiriakidis G, Katsarakis N, Bender M, Gagaoudakis E, Cimalla V. InOx thin films, candidates for novel chemical and optoelectronic applications. *Materials Physics and Mechanics* 2000; 1(2): 83-98.

Layek RK, Nandi AK. A Review on synthesis and proper ties of polymer functionalized graphene. *Polymer* 2014; 54(19): 5087-5103.

McCrum NG, Bucknall CP. *Principles of polymer Engineering*, (2nd ed), Oxford University press Inc, New York 1997.

Naser BA, Nooralhuda JA, Abdulazeez OM. Effect of Solvents on Linear Optical Properties for Nematic Liquid Crystals. *IOP Conference Series: Materials Science and Engineering* 2020: 928(7).

Nnabuchi MN. Optical and solid state characterization of optimized manganese sulphide thin films and their possible applications in solar energy. *The Pacific Journal of Science and Technology* 2006; 7(1): 69-76.

Rasool SR, Al-Zuhairi AJ, Hassan AAM, Mousa AO, Nawfal SH. Synthesis of polymers containing 5,5-dimethylhydantoin and study of its optical properties. *Journal of Global Pharma Technology* 2020; 12(2): 657–663.

Singh V, Kulkarni AR, Rama TR. Dielectric properties of aluminum-epoxy composites. *Journal of Applied polymer Science*, 2003; 90(13): 3602-3608.

Tauc J, Menth A, Wood DL. Optical and magnetic investigations of the localized states in semiconducting glasses. *Physical Review Letters* 1970: 25(11).

Tuama AN, Abass KH, Bin Agam MA. Efficiency enhancement of nano structured Cu_2O:Ag/ laser etched silicon-thin films fabricated via vacuum thermal evaporation technique for solar cell application. *Optik* 2021: 247.

Tuama AN, Abass KH, Agama MA. Fabrication and characterization of Cu_2O: Ag/Si solarc via thermal evaporation technique. *International Journal of Nanoelectronics and Materials* 2020: 13(3).

Walton AK, Moss TS. Determination of refractive index and correction to effective electron mass in PbTe and PbSe. *Proceedings of the Physical Society* 1963; 81(3): 1958-1967.

Wemple SH, Di Domenico Jr. M. Behavior of the electronic dielectric constant in covalent and ionic materials. *Physical Review B* 1971: 3(4).

Abdulrazzak FH, Abass AM, Alkaim AF, Hussein FH. Comparison between chemical vapor deposition and flame fragments deposition techniques for synthesizing carbon nanotubes. *NeuroQuantology* 2020; 18(4): 5-10.